ANNALES
UNIVERSITATIS MARIAE CURIE-SKŁODOWSKA
LUBLIN – POLONIA

VOL. LVII, 15 SECTIO AA 2002

FT-IR/PAS applications in surface science and catalysis[1]

J. Ryczkowski* and S. Pasieczna
Maria Curie-Skłodowska University,
Faculty of Chemistry, Department of Chemical Technology
pl. M. Curie-Skłodowskiej 3, 20-031 Lublin, Poland
tel. +48-81 537-55-96; fax: +48-81 537-55-65;
e-mail: ryczkows@hermes.umcs.lublin.pl

Our concern in this paper is to present basis and the selected examples of the modern spectroscopic technique – FT-IR/PAS (Fourier transform infrared photoacoustic spectroscopy) applications in the surface science and catalytical investigations.
Vibrational spectroscopies are among most widely used methods for the surface characterization. This is because very detailed structural information can be obtained from vibrational spectra. FT-IR/PAS is one of the basic spectroscopic techniques belonging to the conventional optical spectroscopy, and it is an important complimentary method to the other spectroscopic methods applied.

1. INTRODUCTION

The classical definition of a catalyst, in brief, is the following: a catalyst is a substance that changes the kinetics but not the thermodynamics of a chemical reaction. Another definition of a catalyst is more informative: a catalyst is a substance that transforms reactants into products, through an uninterrupted and repeated cycle of elementary steps in which the catalyst participates while being regenerated in its original form at the end of each cycle during the life of the catalyst [1].

The chemistry of catalysis is as varied as chemistry itself. This subject cover many disciplines: surface science; inorganic, organic, and organometallic

[1] This work was presented as plenary lecture during 7th Workshop on Photoacoustics and Photothermics (Ustroń – Beskidy Mountains 2002.02.28 – 2002.03.01).

chemistry; physical chemistry and spectroscopy; theoretical chemistry; materials science; modeling and molecular graphics; and catalytic reaction engineering (Figure 1).

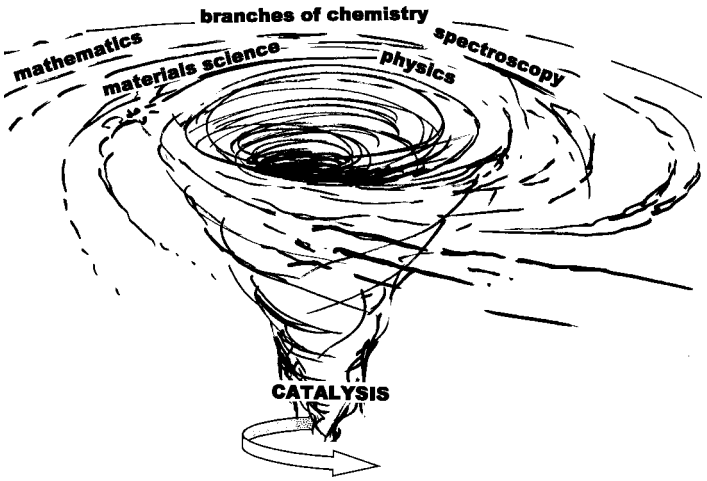

Fig. 1. Catalysis as an interdisciplinary science

Catalysis plays a key role in nature and society since almost every reaction requires a catalytic material. Monitoring the events taking place in such materials is crucial for understanding the reaction mechanisms of many important chemical processes and would allow the rational design of new or better catalytic solids. This monitoring includes the observation of reaction intermediates, the discrimination between spectator species and active sites, the quantification of unusual oxidation states and coordination environments of metal ions in catalyst materials as well as the migration and mobility of species at the catalyst surface. This is the field of *in situ* spectroscopy where *in situ* refers to the study of catalytic materials at their working place under real reaction conditions; *e.g.*, in a gas stream of reactants and at high temperatures. Researchers are nowadays working to develop analytical tools that allow them to follow the physicochemical processes taking place in an active catalyst in real time and under operating conditions; *i.e.*, they are using *in situ* characterization techniques to understand the working of catalyst materials (Figure 2).

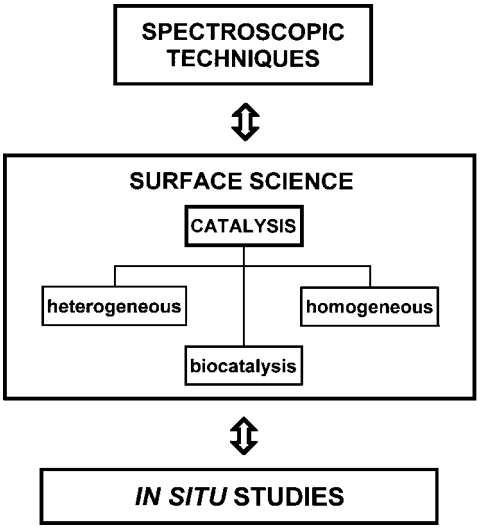

Fig. 2. The correlation between surface science investigations by the spectroscopic techniques

Catalysis is primarily an applied science, however, and as such should reasonably be expected to provide major assistance in reaching the goals of better catalysts and improved catalytic processes, from a better fundamental understanding of catalyst surface chemistry. This is an area in which IR will undoubtedly make further major contributions (Figure 3).

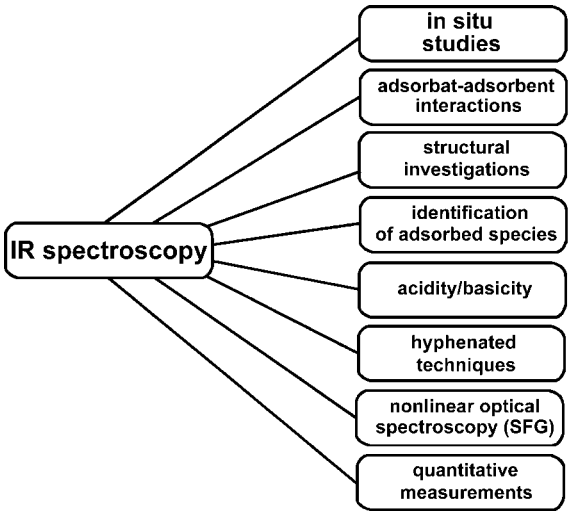

Fig. 3. Application of IR in catalysis and surface science [2]

Vibrational spectroscopies are among the most promising and most widely used methods for catalyst characterization. This is because very detailed structural information can be obtained from vibrational spectra. After nearly 60 years of intensive application, infrared spectroscopy (IR) remains the most widely used, and usually most effective, spectroscopic method for characterization of surface chemistry of heterogeneous catalysts [2-4]. From the historical point of view both catalysis and IR spectroscopy are of the same "age". Scientific bases for those both scientific areas were created at the beginning of XIX century, and since 1940 they are successfully "co-operating" together [2]. In the past few years one can observe a growing interest in the application of IR techniques in catalytic investigations. One of the reasons, among the others, is their wide distribution (nowadays, IR and/or FT-IR spectrometers belong to the standard equipment of each scientific laboratory) and the relatively low costs (compared to the other modern physicochemical techniques for surface characterization) of the base instrument.

A variety of IR techniques has been and can be used in order to obtain information on the surface chemistry of different solids (Figure 4).

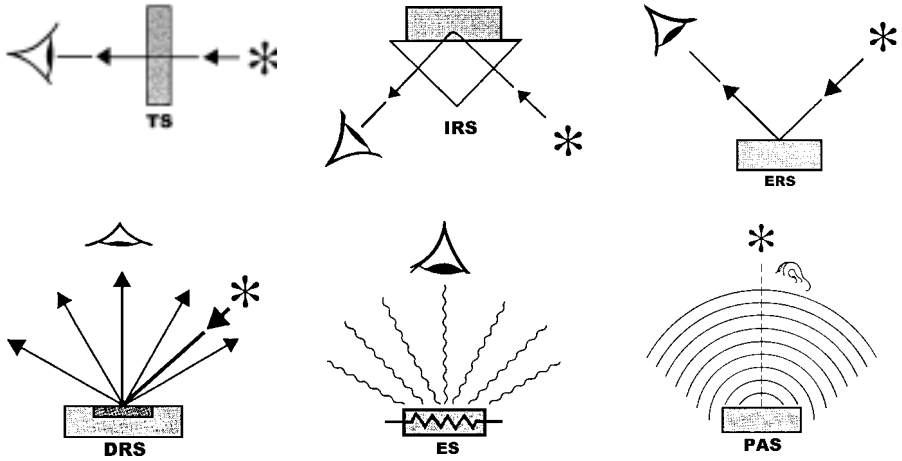

Fig. 4. Basic spectroscopic techniques: TS - transmission spectroscopy, IRS - internal reflection spectroscopy (or attenuated total reflectance – ATR), ERS - external reflection spectroscopy, DRS – diffuse reflectance spectroscopy, ES – emission spectroscopy, PAS - photoacoustic spectroscopy [5]

Special meaning have investigations carried out under the reaction conditions. In principle for *in situ* measurements, almost all forms of IR spectroscopy are suitable. For most practical experimental reasons, however, the transmission-absorption and diffuse reflectance techniques are best suited. This

is more related to the design of cells that are to be used as reactor, than with the principal problems of the other techniques [2-3].

2. GENERAL CONSIDERATIONS

In the broadest sense, spectroscopy can be defined as the study of the interaction of energy with matter. The energy used in optical spectroscopy exists in form of optical photons or quanta, with wavelengths ranging from less than 1 Ångstrom in the x-ray region, to more than 10^6 Å in the far-infrared (FIR). Because of its versatility, range, and non-destructive nature, optical spectroscopy remains a widely used and most popular tool for investigating and characterizing the properties of matter. Conventional optical spectroscopies tend to fall into two major categories. The first category involves the study of the optical photons that are transmitted through the material of interest, that is, the study of those photons that did not interact with the material. The second category involves the study of the light that is scattered or reflected from the material, that is, those photons that have undergone some interaction with the material. Almost all conventional optical methods are variations on these two basic techniques. As such, they are distinguished not only by the fact that optical photons constitute the incident energy beam, but also by the fact that the data are obtained by detecting some of these photons after the beam has interacted with the matter or material under investigation. It should be noted that these optical techniques preclude the detection and analysis of those photons that have undergone an absorption, or annihilation, interaction with the material, even though this process is often the one of most interest to the investigator.

Transmission spectroscopy – TS (Figure 4) is the simplest sampling technique in IR spectroscopy and is used for routine spectral measurements. A small amount, usually 1-3 mg, of finely ground solid sample is mixed with approximately 400 mg powdered potassium bromide and then pressed in an evacuated die under high pressure [2]. The resulting discs are transparent and yield good spectra. The vast majority of experiments are currently performed in the transmission-absorption mode. The fundamentals of the different IR spectroscopic techniques are briefly outlined in view of their use of the studies of oxide heterogeneous catalysts [6].

Photoacoustic spectroscopy (PAS) measures a sample's absorbance spectrum directly with a controllable sampling depth and with little or no sample preparation. This rapid direct analysis capability is applicable to nearly all samples encompassing a wide range of absorbance strengths and physical forms. Among the other key features of PAS are that it is non-destructive, noncontact, applicable to macrosamples and microsamples, insensitive to surface morphology. It has a spectral range from the UV to far-IR, and is

operable in photoacoustic absorbance, diffuse reflectance, and transmission modes; and is capable of measuring spectra of all types of solids without exposure to air or moisture [7,8]. A commercial photoacoustic detector, which operates with all FT-IR manufacturers' instruments, is available (Figure 5) [9].

a) **b)**

Fig. 5. Commercial PAS detector MTEC300: a) front and b) side view [9]

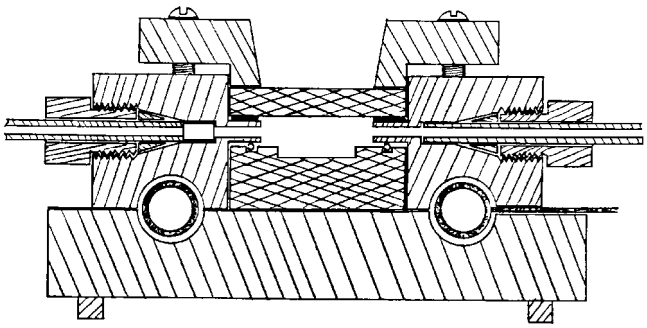

Fig. 6. Scheme of high-temperature PAS sample cell [10]

There are no commercial reactor cells for *in situ* studies, which can operate under FT-IR/PAS measurements. It can be find single examples of such "home made" reactors (Fig 6) [10].

Besides a commercial photoacoustic detector, *e.g.*: MTEC300 (Figure 5), laboratory prototypes can be found in the literature (Figs. 7 and 8) [11,12].

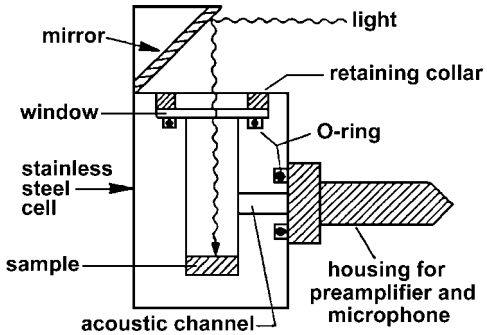

Fig. 7. Schematic diagram of photoacoustic cell for solid samples [11]

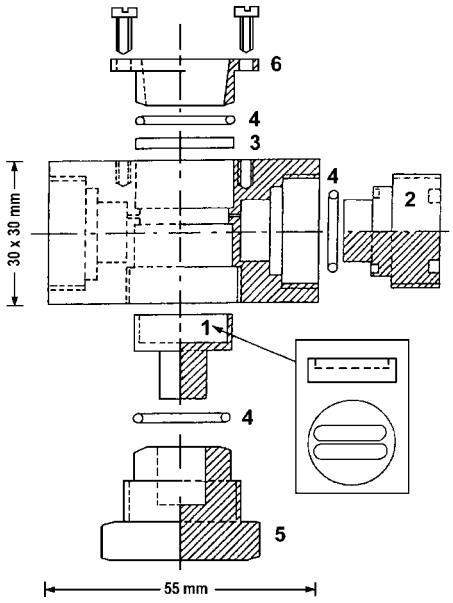

Fig. 8. Photoacoustic sample chamber: 1 – sample cup (holder for sample and reference shown on the insert), 2 – microphones (only one shown), 3 – sapphire window, 4 – O-rings, 5 – bottom screw, 6 – top ring [12]

Photoacoustic spectroscopy is detecting a sample's IR spectrum by "listening" to the sound made when the sample absorbs IR radiation. A highly sensitive microphone is used as a detector, and the spectra are similar to absorbance spectra. This technique can be used for quantitative analysis. Carbon black is commonly used a reference material. What you cannot see or see through you can sometimes hear. That is the idea behind PAS [13].

The photoacoustic signal generation sequence is shown schematically in Figures 9 and 10. Figure 9 shows the IR beam intensity incident on the sample with intensity I_0. The beam intensity is modulated at frequencies, $f = v\nu$, by the FT-IR interferometer when the mirror moves with optical path difference velocity v resulting in a unique modulation frequency corresponding to each wavenumber ν (Figure 9).

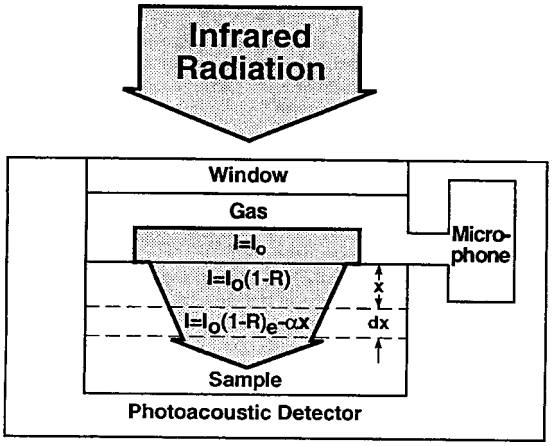

Fig. 9. Schematic of photoacoustic signal generation showing the IR beam intensity changes upon reflection and absorption by the sample [8]

After the IR beam passes through the detector window and a transparent gas (typically He), a fraction, R, is reflected at the sample surface. The IR beam intensity is given by $I_0(1\text{-}R)$ at a depth $x = 0$ inside the sample and decays to a value $I_0(1\text{-}R)e^{-\alpha x}$ at depth x due to absorption of IR radiation in the sample which has absorption coefficient α.

Each layer dx of the sample that absorbs IR radiation experiences an oscillatory heating at frequencies f with temperature change amplitudes, ΔT, proportional to $I_0(1\text{-}R)\alpha e^{-\alpha x}dx$ as shown in Figure 10.

Each sample layer that oscillates in temperature is a source of thermal-waves. In the one-dimensional energy flow schematic of Figure 10, thermal-waves propagate from the sample bulk to the irradiated surface and into the adjacent gas. During propagation, thermal-waves decay with a coefficient $a_s = (\pi f/D)^{1/2}$ where D is the sample thermal diffusivity. Consequently, the surface temperature oscillation amplitude ΔT_s is proportional to $I_0(1\text{-}R)\alpha e^{-(\alpha+a_s)x}dx$ for a thermal-wave generated at depth x just before it crosses into the gas adjacent to the sample surface. A fraction, R_t, of the thermal-wave is reflected back into the sample at the surface resulting in a temperature oscillation amplitude in the gas ΔT_g proportional to $I_0(1\text{-}R)(1\text{-}R_t)\alpha e^{-(\alpha+a_s)x}dx$.

The photoacoustic signal is generated by thermal expansion of the gas caused by heat associated with the sum of all of the ΔT_g contributions. Contributions come from each of the sample layers in which energy of the IR beam is absorbed and which is close enough to the surface so that thermal-wave amplitude has not decayed to a vanishing contribution after crossing the sample-gas interface [8].

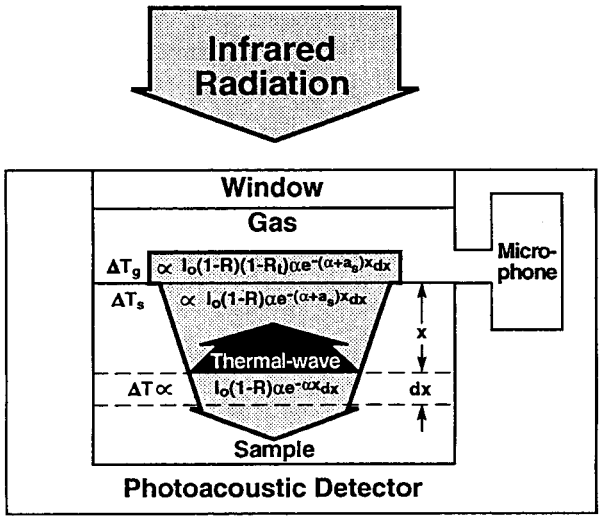

Fig. 10. Schematic of one-dimensional photoacoustic signal generation showing the temperature changes that occur in the sample and adjacent gas [8]

Optical spectroscopy has been a scientific tool for over a century, and it has proven invaluable in studies on reasonably clear media, such as solutions and crystals, and on specularly reflective surfaces. There are, however, several instances where conventional transmission spectroscopy is inadequate even for the case of clear, transparent materials. Such a situation arises when one is attempting to measure a very weak absorption, which in turn involves the measurement of a very small change in the intensity of a strong, essentially unattenuated, transmitted signal. Although this problem occurs for all forms of matter, it has received particular attention in the case of transparent gas mixtures containing minute quantities of an absorbing species or pollutant. Various techniques developed to overcome this difficulty, such as derivative spectroscopy, have proven to be generally inadequate.

In addition to weakly absorbing materials, there are a great many nongaseous substances, bath organic and inorganic, those are not readily amenable to the conventional transmission or reflection modes of optical spectroscopy. These are usually highly light-scattering materials, such as

powders, amorphous solids, gels, smears, and suspensions. Other difficult materials are those that are optically opaque and have dimensions that far exceed the penetration depth of the photons. In the former case, the optical signal is composed of a complex combination of specularly reflected, diffusely reflected, and transmitted photons, making the analysis of the data extremely difficult. In the latter case, the absorptive properties of the material are difficult, if not impossible, to determine, since essentially no photons are transmitted. Over the years, several techniques have been developed to permit optical investigation of highly light-scattering and opaque substances. The most common of these are diffuse reflectance (*e.g.,* DRIFT – diffuse reflectance Fourier transform IR spectroscopy), attenuated total reflection (ATR), internal reflection spectroscopy (IRS), and Raman scattering (RS) [2,14,15]. All these techniques have proven to be very useful, yet each suffers from serious limitations. In particular, each method is applicable to only a relatively small category of materials, each is useful only over a small wavelength range, and the data obtained are often difficult to interpret.

During the past thirty years, another optical technique has been developed to study those materials that are unsuitable for the conventional transmission or reflection methodologies. This technique, PAS, is different than the conventional techniques chiefly in that even though the incident energy is in the form of optical photons, the interaction of these photons with the material under investigation is studied not through subsequent detection and analysis of some of the photons, but rather through a direct measure of the energy absorbed by the material as a result of its interaction with the photon beam.

3. SELECTED EXAMPLES

One of the major advantages of PAS is its relative immunity to scattered light. Consequently, this methodology can provide absorption spectra of highly light-scattering materials such as powders, *e.g.*: alumina, silica [16-19]. Most infrared studies have been performed by transmission techniques using thin pressed discs in the region where silica and alumina are IR transparent, typically in the regions above 1400 cm-1 and between 500 and 1000 cm-1 for silica and above 1200 cm-1 for alumina (Figure 11).

Several of the problems associated with transmission techniques may be overcome utilizing photoacoustic detection. In particular, changes in the spectral region where silica and alumina are strong absorbers may be observed by PAS. The main advantages and disadvantages of transmission and photoacoustic spectroscopies are summarized in Table 1 [21].

The only noticeably difference between “b” (as received) and “a” (dried) is a broad band due to adsorbed water (the negative feature at 1008 cm^{-1} – “d” appears to be due to an Si-OH stretching mode; this feature is red shifted to

926 cm^{-1} when water is adsorbed). In the case of sample "c" – this treatment initiates gel formation, so that the sample is no longer a chain of silica particles held together by electrostatic forces, but a porous network held together by siloxane linkages. The most obvious features in this spectrum are an increase in the water adsorption at 3400 and 1632 cm^{-1}. In addition, a band at 976 cm^{-1} is evident, that was much less obvious in the two earlier spectra. This feature is due to siloxane bridges formed during gel formation.

Fig. 11. IR spectra in the region 1800-500 cm^{-1} for: a) SiO_2, b) γ-Al_2O_3 [20]

Tab. 1. A comparison of transmission and photoacoustic spectroscopies [21]

	Transmission	photoacoustic
sample preparation	pressed disc or mull	loose powder
effect of scattering	can cause spectral distortion	negligible
Spectrum acquisition time	Seconds	seconds
spectral region probed	Limited to 4000-1200 cm^{-1} from absorption by lattice modes of solid	4000-400 cm^{-1} only spectral limitations are imposed by spectrometer
Special problems	reflection losses result in low optical throughput limiting signal to noise	highly susceptible to airborne noise and building vibrations
in situ investigations	possible	almost impossible

Photoacoustic spectra of a variety of silica samples are shown in Figure 12.

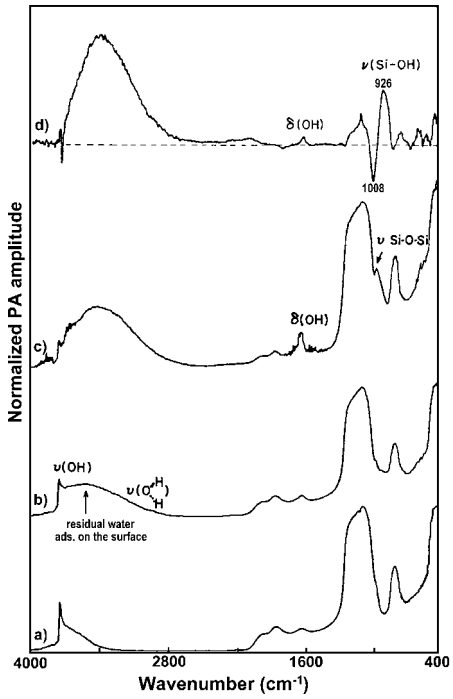

Fig. 12. FT-IR/PAS spectra of: a) Aerosil dried at 350 ^{o}C, b) Aerosil as received, c) Aerosil slurried in water and dried at 100 ^{o}C, d) difference spectrum (b – a) [21]

Alumina forms a variety of oxides and hydroxides [22]. From the catalytic viewpoint γ-Al_2O_3 is the most important. This is a metastable phase that is

produced from successive dehydration of aluminium trihydroxide (gibbsite) to aluminium oxide hydroxide (boehmite) to γ-alumina, or from dehydration of boehmite formed hydrothermally. γ-Al_2O_3 is converted into α-Al_2O_3 (corundum) at temperatures around 1000°C.

The infrared spectra for various aluminum oxides and hydroxides are shown in Figure 13.

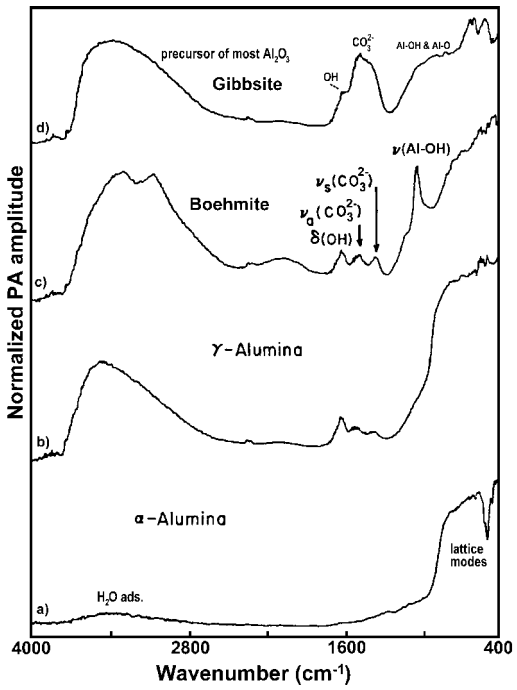

Fig. 13. FT-IR/PAS spectra of aluminium oxides and hydroxides: a) α-Al_2O_3 (4 m^2/g), b) γ-Al_2O_3 (234 m^2/g), c) Boehmite - AlO(OH) (325 m^2/g), d) Gibbsite – $Al(OH)_3$ [21]

Figure 13a is α-Al_2O_3, ground to a fine powder with a surface area of 4 m^2/g. The absorption between 550 and 900 cm^{-1} is due to two overlapping lattice modes, and the low frequency band at 400 cm^{-1} is due to another set of lattice vibrations. There is also a very weak and broad band at 3400 cm^{-1} due to water adsorbed on the alumina surface. As the surface area is low this band is not expected to be very strong.

Figure 13d is the IR spectrum of gibbsite, which is the precursor of most aluminum oxides. The spectrum shows a broad band due to OH stretches at 3400 cm^{-1}, a feature centered around 1510 cm^{-1} due to carbonate, and a shoulder at 1632 cm^{-1} due to OH bending of water. The A1-OH or A1-O stretching

modes give rise to a broad band that begins to absorb strongly at 1250 cm^{-1} and extends to below 400 cm^{-1}. There are smaller absorption bands at 668, 634, and 556 cm^{-1} superimposed on the broad A1-O band, which appear to be due to bending modes of carbonates. Since gibbsite is produced by precipitation from a basic solution buffered with sodium carbonate the high water and carbonate contents observed are not unexpected.

Dehydration of gibbsite under pressure in moist air produces boehmite (aluminum oxide mono-hydrate). An IR spectrum of boehmite is shown in Figure 13c. When the gibbsite is dehydrated a structural collapse occurs with a large increase in surface area. The boehmite sample has a nominal surface area of 325 m^2/g. The IR spectrum of the boehmite shows distinct structure in the OH stretching region, with two peaks located at 3090 and 3320 cm^{-1}. There are three features at 1648, 1516 and 1392 cm^{-1} that are due to adsorbed water and carbonate, which are removed upon heating the boehmite to 350°C in hydrogen. The lattice vibrations begin to absorb strongly below 1200 cm^{-1}. An additional feature at 1072 cm^{-1}, characteristic of boehmite, is the result of the A1-OH stretch. Further dehydration of boehmite at 600°C produces γ-Al_2O_3, whose spectrum is shown in Figure 13b. There is a loss in surface area in going from boehmite to γ-Al_2O_3. The sample shown here has a surface area of 234 m^2/g. The γ-alumina sample shows two major differences from α-alumina. First, there is a more intense broad absorption band at 3400 cm^{-1} due to adsorbed water on the γ-Al_2O_3. Second, the γ-alumina does not show splitting of the phonon bands between 400 and 500 cm^{-1} as was observed for α-Al_2O_3. The γ-alumina is a more amorphous structure and has much smaller crystallites so the phonon band is broader. The γ-Al_2O_3 also shows three features at 1648, 1516 and 1392 cm^{-1} due to adsorbed water and carbonate.

Figure 14 shows a series of difference spectra for adsorption on γ-alumina. Spectra were taken after drying the γ-Al_2O_3 at 350 ^oC, cooling to room temperature (RT) and carrying out RT adsorption. The spectra are the difference of the sample before and after adsorption.

Spectrum 14e is the spectrum for the as received alumina differenced with the dried alumina. The positive band at 3400 cm^{-1} is due to adsorbed water, and the small negative feature at 3740 cm^{-1} is due to isolated hydroxyls on the dried surface [22-29]. Besides the three features previously noted at 1644, 1516 and 1392 cm^{-1}, there are features at 1074 cm^{-1} due to an Al-OH_2 stretch of co-ordinatively bound water, and small features at 748 and 628 cm^{-1}. Spectrum 13a is for CO_2 adsorption. The gas phase CO_2 shows bands at 2346 and 668 cm^{-1}; bands at 1654, 1436 and 1228 cm^{-1} are due to adsorbed bicarbonate species. There is a weak band at 3610 cm^{-1} due to the OH stretch in the bicarbonate that is accompanied by small negative features at 3740 cm^{-1} corresponding to the hydroxyl that reacted to form the bicarbonate.

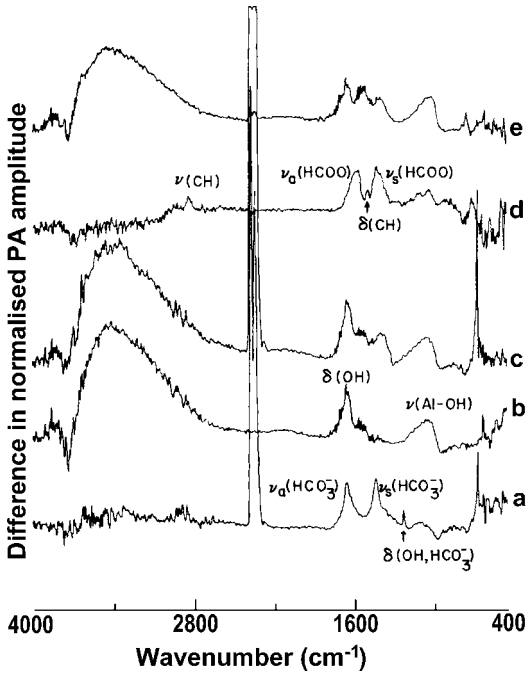

Fig. 14. Difference spectra of adsorbed species on γ-alumina (air exposure): a) CO_2, b) H_2O, c) H_2O followed by CO_2, d) methanol reacted with the alumina at 350 °C, e) as received γ-alumina (air exposure) [21]

A weak band at 1050 cm^{-1} is due to the C-O stretch in the bicarbonate. The bicarbonate bands disappear when the sample is exposed to water. After exposure of the γ-alumina sample to water several features are apparent in the infrared spectrum (Figure 14b) that were also apparent in the spectrum of the as received sample. An OH bending mode for adsorbed water appears at 1644 cm^{-1}, as well as an Al-OH_2 stretching mode at 1058 cm^{-1} and another feature at 628 cm^{-1} that is probably due to a frustrated rotation of the adsorbed water. When the surface with adsorbed water is exposed to CO_2 additional features appear at 1536 and 1384 cm^{-1}, as shown in Figure 14c. A small feature also starts to grow at 748 cm^{-1}. These results suggest that a monodentate carbonate ligand is formed when CO_2 adsorbs on the alumina surface with water adsorbed. The features at 1536 and 1384 cm^{-1} are due to the asymmetric and symmetric stretches respectively. The C-O stretching mode that occurs around 1050 cm^{-1} coincides with the A1-OH_2 stretch. The feature at 748 cm^{-1} corresponds to the out-of-plane deformation of the carbonate. A feature due to the planar deformation appears as a high -frequency shoulder on the water libration at 628 cm^{-1}. A shoulder also forms on the water band at 3620 cm^{-1}, which is also visible in the as received alumina. This is the position for the OH

stretch in a bicarbonate. However there is no evidence for the OH bending mode at 1230 cm^{-1}, suggesting that the carbonate interacts with adsorbed water, but does not react to form a bicarbonate species [21].

The carbonate can also be compared with adsorbed formate species prepared by reacting methanol with the alumina surface at 350°C. The spectrum for adsorbed formate, Figure 14d, shows the asymmetric carboxylate stretches at 1565 and 1440 cm^{-1} respectively, the CH stretch at 2832 cm^{-1}, and the CH bending mode at 1505 cm^{-1}. The A1-OC stretching mode is seen at 1060 cm^{-1}, and the out-of-plane deformation at 750 cm^{-1}. The signal to noise ratio in the low frequency end of the spectrum is insufficient to see the planar deformation, which should occur around 630 cm^{-1}. It should be noted that the carbonate and formate species are very similar, the main distinction being the vibrations associated with the CH bond [21].

In a recent study, series of chromia materials were prepared from CrO_3 and C_1-C_4 alcohols [30]. Under non-oxidative conditions acetate species show remarkable thermal stability. Bands observed in the 1050-900 cm^{-1} region of thermally treated samples are characteristic for chromia being in a nearly stoichiometric state, indicating that re-oxidation of the partially reduced samples occurred when they were exposed to ambient air. When the samples are treated under oxidative conditions carboxylate species are completely decomposed at 450 ^{o}C. Surface area is reduced considerably due to the crystallization of α-Cr_2O_3. In FT-IR/PAS spectra sharp bands at 994 and 978 cm^{-1} characteristic for C=O stretching in chromate species, indicate the formation of non-stoichiometric oxide with excess of oxygen.

McGovern *et al.* [10] have studied methanol adsorption on silica and Na-Y zeolites. A partially dried Na-Y sample was prepared by heating to 150 ^{o}C for 4 h in flowing helium, cooled to RT, than exposed to 100 Torr of methanol for 15 min (Figure 15).

Figure 15a shows that prior to methanol exposure there is a sharp absorption feature at 3695 cm^{-1}, probably associated with the hydrated cation of a surface hydroxide. After RT adsorption of methanol spectrum 15b shows that the peak at 3695 cm^{-1} is replaced by C-H stretching features at 2950 and 2840 cm^{-1}. Two bands at 1460 and 1400 cm^{-1} are found in the C-H bending region together with broad features in the Si-O and C-O stretching region.

Nishikawa *et al*. [31] has studied the interaction of gamma-iron oxide powder with several substances, *e.g.*: stearic acid (SA). Figure 16 shows the FT-IR/PAS spectrum with the γ-Fe_2O_3.

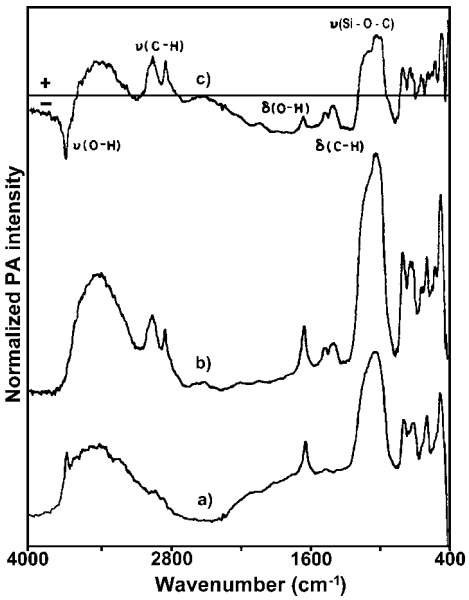

Fig. 15. FT-IR/PAS spectra of methanol adsorption on NaY zeolite: a) with CH_3OH adsorption at 20 °C and purged in He, b) zeolite dried at 150 °C, c) difference spectra (a – b) [10]

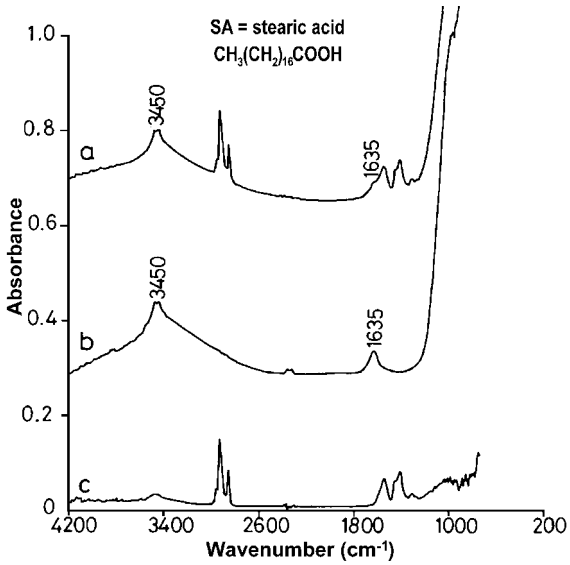

Fig. 16. FT-IR/PAS spectra of: a) SA on γ-Fe_2O_3 powder, b) γ-Fe_2O_3 powder itself, c) the difference spectrum (a-b) [31]

The upper spectrum is the composite of oxide/SA; the middle spectrum is that of the gamma-iron oxide. As shown in Figure 16a, SA adsorbed on the gamma-iron oxide is clearly observed at around 2900-2800 cm^{-1} and 1500-1400 cm^{-1}. However, absorption due to water adsorbed onto the oxide was also visible at around 3450 and 1635 cm^{-1}. Since the adsorbed-water absorption at 1636 cm^{-1} hampers the identification of SA absorption due to the carboxyl group observed at 1700 cm^{-1}, the water absorption was subtracted. As is clear from Figure 16c, such a subtraction of the absorption of the water and that of the gamma-iron oxide is readily accomplished.

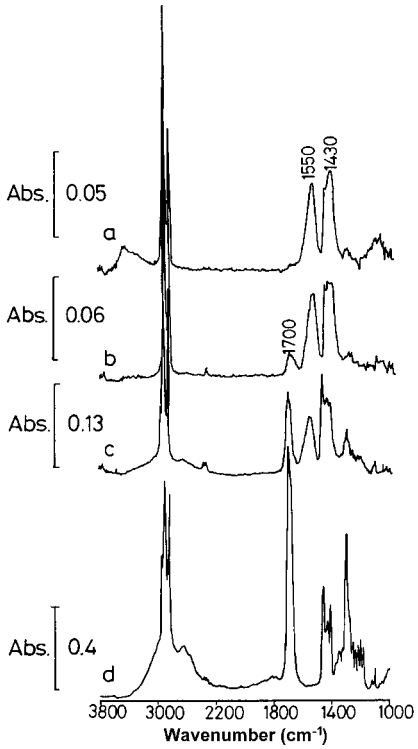

Fig. 17. FT-IR/PAS spectra of SA on γ-Fe_2O_3 powder treated with various concentrations of SA solution after subtraction of the oxide itself: a) 0.1%, b) 0.2%, c) 0.5% and of d) the SA itself without the oxide [31]

The spectrum of SA on gamma-iron oxide treated with 0.1% SA solution (Figure 17a) is very different from that of SA without the oxide (Figure 17d). Two bands (1550 and 1430 cm^{-1}) were clearly identifiable, while the band at 1700 cm^{-1} corresponding to the carboxyl group was completely missing. These bands are assigned to the antisymmetric and the symmetric COO^- stretching vibration, respectively, indicating that the SA was chemisorbed onto the

gamma-iron oxide through the carboxyl group and dissociated the proton in the carboxyl group. With increasing concentration of the SA solution, the absorption at 1700 cm^{-1} due to the free-state or physically adsorbed carboxyl group clearly increased (Figure 17b and 17c), suggesting that the chemisorbed site at the gamma-iron oxide was lost.

The interaction of EDTA (ethylenediaminetetraacetic acid) and its salt with γ-Al_2O_3 surface is the next example of FT-IR/PAS application (Figure 18).

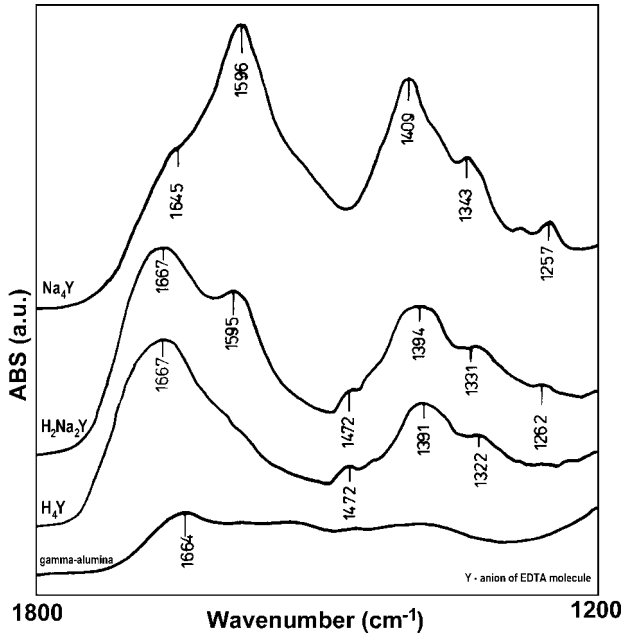

Fig. 18. FT-IR/PAS spectra of EDTA adsorbed on γ-Al_2O_3 [32]

Results were compared with those obtained by the classical transmission method. Spectroscopic data are summarized in Table 2.
Detailed description of the studies done can be found elsewhere [32].

Hess and Kemnitz [33] have applied FT-IR/PAS investigations for surface acidity and catalytic behavior of modified zirconium and titanium dioxides (Figs. 19 and 20).

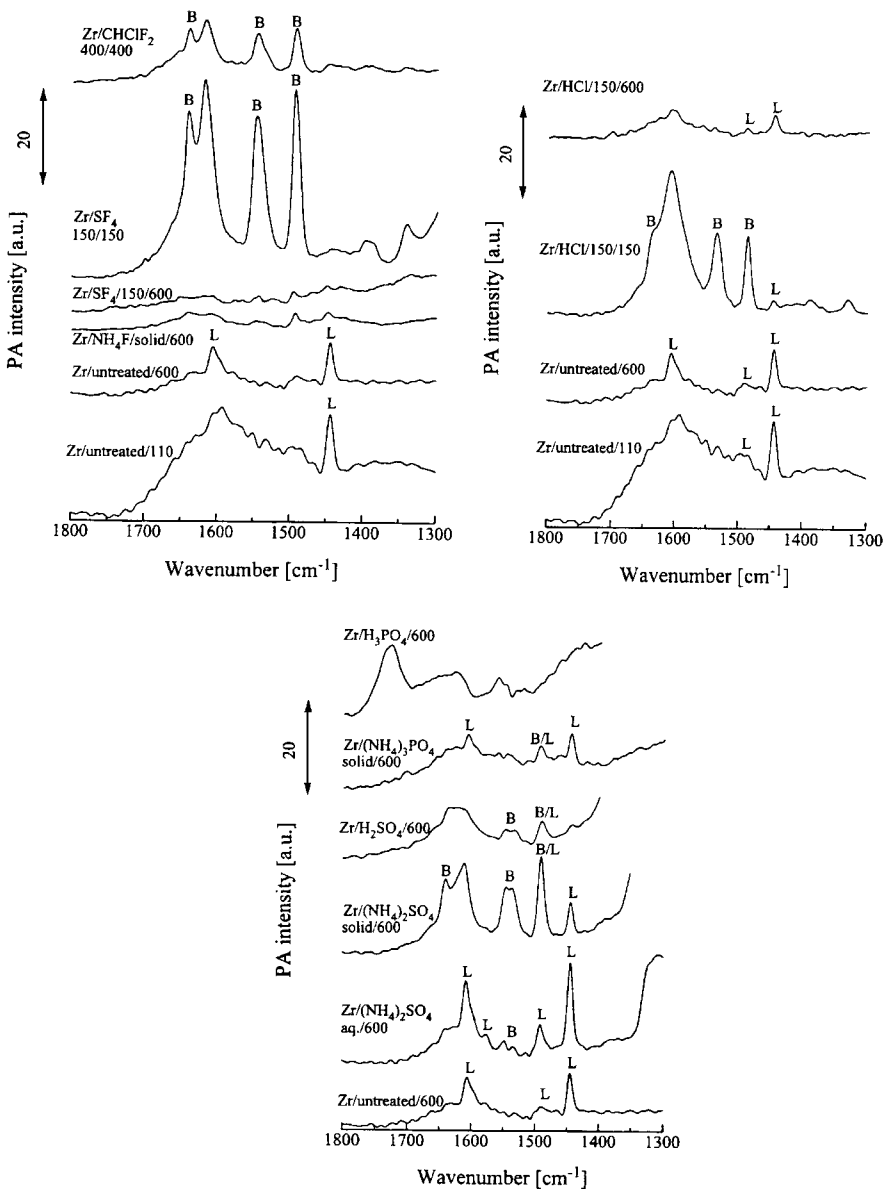

Fig. 19. FT-IR/PAS spectra of pyridine chemisorbed on modified ZrO_2 samples (L, B – pyridine chemisorbed on Lewis and Brønsted acid sites, respectively) [33]

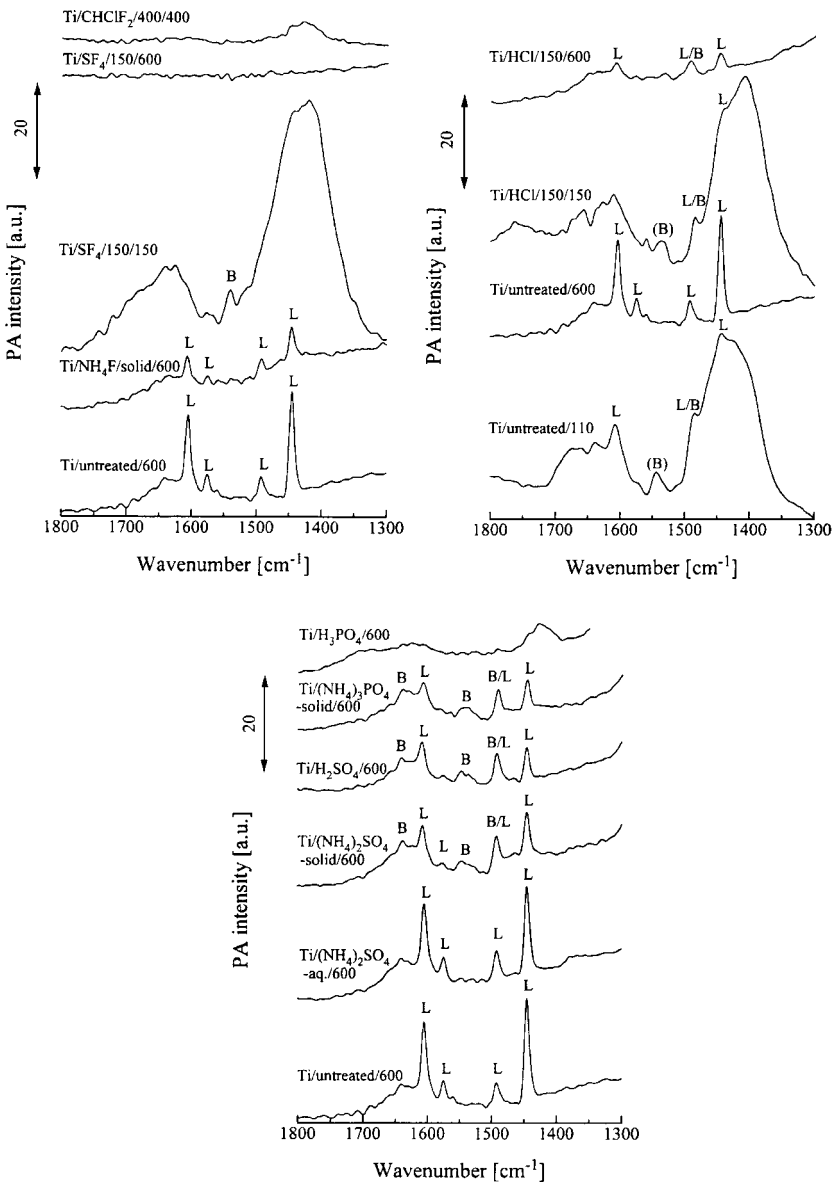

Fig. 20. FT-IR/PAS spectra of pyridine chemisorbed on modified TiO_2 samples (L, B – pyridine chemisorbed on Lewis and Brønsted acid sites, respectively) [33]

The nature of acid sites was determined by FT-IR/PAS of pyridine adsorption and correlated with the catalytic behavior. Those studies are the continuation of those carried out earlier where in a similar way the acidity of γ-Al_2O_3, α-Cr_2O_3 and β-AlF_3 samples was determined [34].

Tab.2. Selected band positions (cm^{-1}) and assignments in recorded spectra [32]

EDTA	C=O	COO^-	$(C\text{-}H)CH_2$	COO^-	NH^+	COO^-
H_4Y						
Unadsorbed	1685		1450	1423	1390	1344
FT-IR	1665		1469		1385	1328
FT-IR/PAS	1667	1595	1472		1391	1332
H_2Na_2Y						
Unadsorbed	1672	1625	1475	1395	1392	1315
FT-IR	1689	1601	1471	1409		1336
FT-IR/PAS	1667	1595	1472	1394		1331
Na_4Y						
Unadsorbed		1596		1411		1329
FT-IR	1664	1596		1417		1342
FT-IR/PAS	1645	1596		1409		1343

Structural and acidic properties of copper-silica catalysts were studied by differential scanning calorimetry (DSC) and FT-IR/PAS [35]. Pyridine was used as a molecular probe for determining the concentration of acid sites present on the surface of oxide catalyst. Those studies were extended for bimetallic systems supported on silica [36]. Pyridine adsorption was used to study the acidic sites of $CuO\text{-}MoO_3/SiO_2$, with reference to CuO/SiO_2 and MoO_3/SiO_2 catalysts (Figs. 21 and 22).

There are six major bands for 1 wt. % Cu – 9 wt. % Mo/SiO_2 sample (Figure 21a) at 1636, 1538, 1608, 1574, 1487 and 1450 cm^{-1} (these correspond to the bands of pyridine adsorbed on Lewis and on Brønsted acid sites). As the copper loading is increased (Figure 21 a-d), major changes in the bands occur. The disappearance of the band at 1537 cm^{-1} is accomplished starting from 6.6 wt. % of copper (Figure 21c). Whereas the band at 1636 cm^{-1} is significantly decreased and shows a shift to a lower wavenumber, 1632 cm^{-1}, upon increasing the wt. % of copper. Furthermore, the strong band at 1487 cm^{-1}, which represents both Lewis and Brønsted acidity, observed in both CuO/SiO_2 and MoO_3/SiO_2 catalysts, shows a significant decrease as a result of increasing the Cu loading.

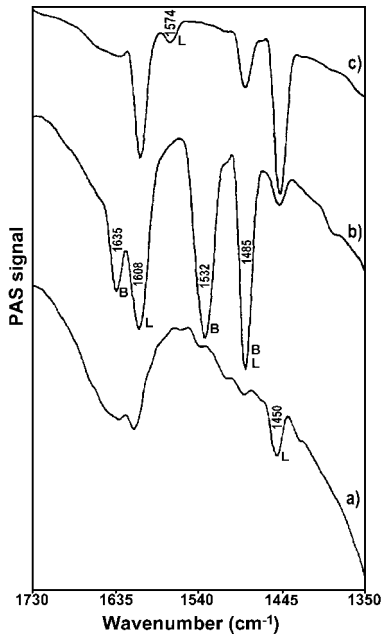

Fig. 21. FT-IR/PAS spectra of pyridine adsorbed at 393 K on the following catalysts supported on silica gel: a) 9 wt. % CuO/SiO_2, b) 9 wt. % MoO_3/SiO_2, c) 9 wt. % CuO - 9 wt. % MoO_3/SiO_2 [36]

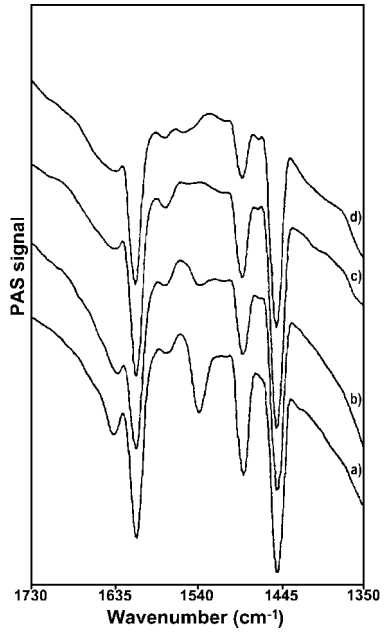

Fig. 22. FT-IR/PAS spectra of pyridine adsorbed at 393 K on oxidized catalysts supported on silica gel: a) 1 wt. % CuO - 9 wt. % MoO_3, b) 3 wt. % CuO - 9 wt. % MoO_3, c) 6.6 wt. % CuO - 9 wt. % MoO_3, d) 15 wt. % CuO - 9 wt. % MoO_3 [36]

Figure 22 shows the IR spectra of pyridine adsorbed on 9 wt. % CuO/SiO_2, 9 wt. % MoO_3/SiO_2 and 9 wt. % CuO – 9 wt. % MoO_3/SiO_2 catalysts.

Spectrum of 9 wt. % CuO/SiO_2 catalyst (Figure 22a), shows the band at 1450 cm^{-1}, of a Lewis site, and the band at 1612 cm^{-1} along with a small band at 1488 cm^{-1}.

Spectrum of 9 wt. % MoO_3/SiO_2 catalyst (Figure 22b), generates both Lewis and Brønsted acid sites. The bands at 1635 and 1532 cm^{-1} are assigned to pyridine adsorbed on Brønsted acid sites. The other bands in the spectrum (1608 and 1450 cm^{-1}) are assigned to pyridine adsorbed on Lewis acid sites except the 1485 cm^{-1} band, which represents the contribution of both sites together. It is obvious that the intensity of the bands (either Lewis or Brønsted) in the 9 wt. % MoO_3 sample exceeds that of the 9 wt. % CuO sample. This reflects the enhancement of acid sites for Mo/silica compared with Cu/silica. This increase in total acidity is caused primarily by the increase in Brønsted acidity resulting from the presence of Mo as clusters and layered oxides.

It should be noted also that the 1450 cm^{-1} band intensity (Figs 22a and b) is more important on Cu/silica relative to Mo/silica and the strength of Lewis sites on Cu/silica is much higher than those on Mo/silica since the former is characterized by a band at 1612 cm^{-1} whereas the latter at 1608 cm^{-1}.

Spectrum of 9 wt. % CuO – 9 wt. % MoO_3/SiO_2 sample (Figure 22c), shows bands at 1608, 1574, 1488, and 1450 cm^{-1}. This spectrum reflects a new band at 1574 cm^{-1} of Lewis acidity and the disappearance of 1635 and 1532 cm^{-1} bands of Brønsted acid sites. The band at 1488 cm^{-1} decreases in intensity and shifts to longer wave number compared with the individual supported oxide catalyst. Furthermore, an extensive increase in intensity of the 1450 cm^{-1} band is observed. As is evident from this spectrum, an increase in the number and strength of Lewis acid sites while a decrease of Brønsted acid sites is observed. The terminal double bonded oxygens for Mo are essential for creating Brønsted acid sites. However, any distortion in this environment will induce a great loss in Brønsted acidity. This distortion has been obtained as a result of the involvement of Cu atoms in the Mo/silica structure.

These results suggest that there is a detachment of the Mo species from the SiO_2 support as a result of increasing the Cu loading and this imparts the formation of $CuMoO_4$ species. Therefore, it is likely to attribute the 1574 cm^{-1} band (Figure 22c) of Lewis acidity to the copper-molybdate species.

The system Mo/SiO_2 finds a wide range of applicability in catalysis, *e.g.*: methane, propane and methanol oxidation. Therefore, many physicochemical techniques have been used to investigate the interaction between Mo species and the silica support. Among this techniques IR spectroscopy, which concerned mainly the low frequency region (1100-400 cm^{-1}) is expected to result in bands corresponding to the interacting species (Figure 23) [37].

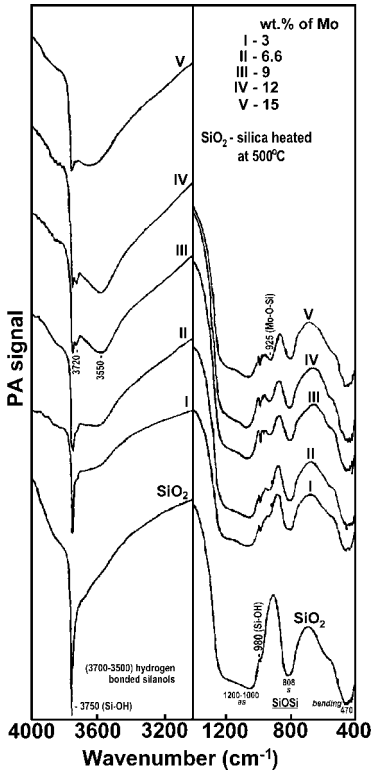

Fig. 23. FT-IR/PAS spectra of parent silica and corresponding samples loaded to different wt. % of Mo [37].

Upon loading with increasing amounts of Mo some new features appear that show dependence on Mo content (Figure 23). Thus bands at 925, 970 and 994 cm^{-1} have appeared which increase in intensity with the increase in Mo loading. These three bands are attributed to Mo-O-Si vibration, terminal Mo=O groups in the surface molybdate phase, and the Mo=O group in the MoO_3 phase, respectively.

Fluorination caused the absence of the band at 970 cm^{-1} up to 12 wt. % of Mo loading, and of the band at 994 cm^{-1} up to 6.6 wt. %, but the appearance of the band at 925 cm^{-1}, at very reduced intensity, in samples I-F and II-F (Figure 24) [37]. In the high frequency region, fluorination resulted in the appearance of a band at 3660 cm^{-1} in addition to the bands at 3750, 3720 and 3550 cm^{-1}, which appeared in the case of unfluorinated samples.

Fluorination usually affects the surface through substitution of some surface hydroxyls by fluoride ions. That means a general decrease in the OH density, which decreases the probability of finding vicinal silanol groups with a geometry that permits easy interaction with interacting Mo species.

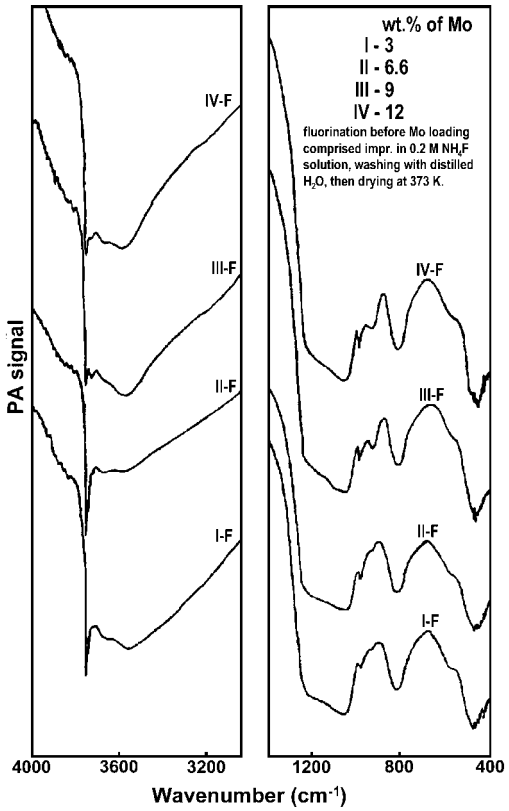

Fig. 24. FT-IR/PAS spectra of prefluorinated Mo/SiO_2 samples [37]

The study of surface characteristics revealed that Mo loading results in a greater decrease in surface area than in pore volume. Thus the narrow pores characterized by a high surface to volume ratio are responsible for these variations. The narrow pores, which accommodate a higher density of suitably situated hydroxyls for interaction with Mo species, represent the most favourable region to be attacked at low levels of Mo loading. The limited space available in these pores in which the interaction with surface hydroxyls and the detachment of weakly bound species took place caused the measured area and volume to decrease progressively with increase in Mo loading. At 15 wt. % Mo the content of interacting species seems sufficient to extend the interaction considerably to the wider pores where the escape of the detached species has mostly occurred. This appears as a relative increase in area and volume. Fluorination has thrown more light on the role of adjacent hydroxyls in narrow pores where the extent of interaction with Mo is decreased, resulting in a corresponding loss of area [37].

The principal advantage of FT-IR/PAS over transmission spectroscopy lies in the determination of vibrational species chemisorbed on opaque, light scattering surfaces [10]. This was demonstrated by obtaining PAS spectra of pyridine chemisorbed on reduced and sulfided Mo/Al_2O_3 and $Co\text{-}Mo/Al_2O_3$ catalysts (Figs. 25 and 26) [10].

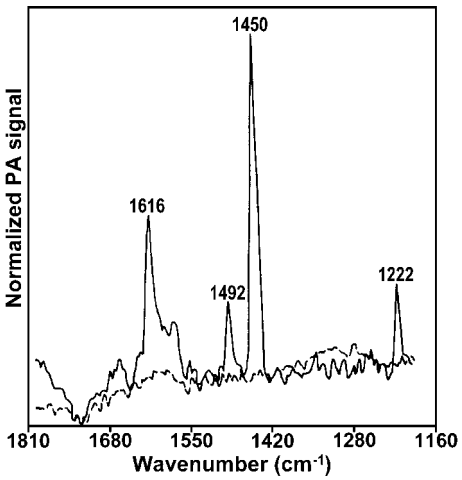

Fig. 25. FT-IR/PAS spectra of sulfided Mo/Al_2O_3 before (dashed line) and after (solid line) exposure to pyridine [11].

The black sulfided samples are opaque at both visible IR wavelengths, but good quality photoacoustic (PA) spectra of these surfaces are readily obtained. Only Lewis acid sites are detected on these surfaces. In addition, the high surface sensitivity of this technique (a small fraction of a monolayer) permits PA detection of a surface cobalt-aluminate type of domain, which is uninfluenced by the presence of molybdenum, is resistant to sulfiding and is capable of adsorbing pyridine. This PA band (at 1315 cm^{-1}) was not observed in transmission studies because such spectral measurements of attenuation of a beam passing through the sample lack the requisitive surface sensitivity [10].

Thermally stimulated desorption of phenylethanol bound by partial carbonisation to silica gel surface was studied (Figure 27) [38].

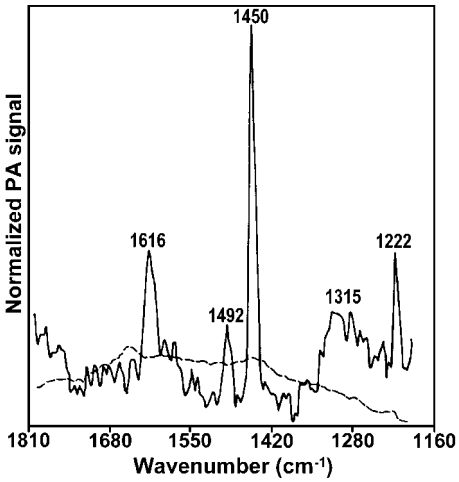

Fig. 26. FT-IR/PAS spectra of sulfided 1.9 wt. % Co – 6.9 wt. % Mo/Al_2O_3 before (dashed line) and after (solid line) exposure to pyridine [11]

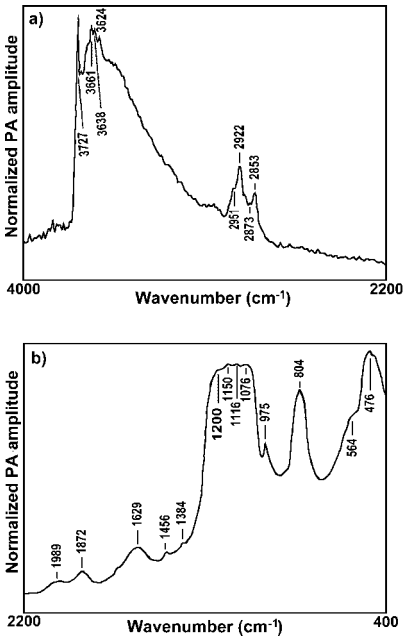

Infrared frequency and band assignement of the recorded spectra

Group	Frequency (cm^{-1})	Assignment
≡Si–OH	3727	νOH
–OH	3700–3000	ν(OH)
CH_3–C	2951	νCH_{3as}
>C CH_2 >C	2922	νCH_{2as}
CH_2–C	2873	νCH_{2s}
>C CH_2 >C	2853	νCH_{2s}
C–H	1989	νC–H
C–H	1872	νC–H
–OH	1629	ν(OH)
>C CH_2 >C	1456	CH_2
Si–O–Si	1300–1000	$\nu Si–O–Si_{as}$
Si–OH	975	νSi–OH
Si–O–Si	804	$\nu Si–O–Si_s$
O–Si–OH	564	O–Si–OH
$-Si(OC_2H_5)_3$	476	νSi–O–C

Fig. 27. FT-IR/PAS spectrum of carbosil sample [38]

According to the data obtained the narrow band at about 3727 cm^{-1} corresponds to free surface hydroxyl groups (isolated Si-OH), and the wide band in the range 3700-3000 cm^{-1} (including resolved vibration at 3661, 3638 and 3624 cm^{-1}) as well as the band at about 1629 cm^{-1} to surface hydroxyl groups bound with physically adsorbed water molecules. In turn, bands at about 2922 and 2951 cm^{-1} are usually attributed to asymmetric stretching vibrations of the C-H bonds in methyl (2920 cm^{-1}) and methylene (2955 cm^{-1}) groups. The two additional bands at 1989 and 1872 cm^{-1} can be attributed to C-H stretching of vinyl compounds or substituted benzenes. However, there are no bands at about 1600, 1650 and 3060 cm^{-1}, and this could be taken as evidence of the absence of polycyclic aromatic compounds in the investigated sample. The band at 1456 cm^{-1} can be assigned to the antisymmetric deformation mode of $-CH_2$ groups. The above data, as well as the presence of bands with maxima at about 2951, 2922, 2873, 2853, 1989, 1872 and 1456 cm^{-1}, support the conclusion that polymeric carbon chains are present on the surface of the adsorbent. The large adsorption feature between 1000 and 1300 cm^{-1} is due to transverse and longitudinal lattice vibration (Figure 11a). The next group of bands (at 975, 804 and 564 cm^{-1}) can be attributed to Si-OH stretching, OH deformation, and O-Si-OH deformation modes, respectively. However, the band at 804 cm^{-1} may also be attributed to Si-O-Si symmetric stretching vibration. The last band shown in Figure 27 with maximum intensity at 476 cm^{-1} can be attributed to Si-O-C vibration.

Activated carbons are particularly useful due to their high adsorption capacity, fast adsorption kinetics and relative ease of regeneration. Due to the interesting applications of activated carbon, a lot of research has been carried out on the preparation of cost-effective adsorbents as a substitute for activated carbon. Hu and Vansant [39] have investigated a new adsorbent prepared by chemical activation of elutrilithe with potassium hydroxide. The changes on the carbon surface with the activation temperature were studied by FT-IR/PAS (Figure 28).

For the sample treated at 500 ^oC, a band at 1600 cm^{-1} could be attributed to the condensed aromatic ring system or to hydrogen-bonded conjugated carbonyl groups or to the interaction of C=C bands, which are polarized by binding of oxygen near one end. A broad band in the 3600-3000 cm^{-1} region is attributed to bridged hydrogen bands. These bonds of C-O or C-C groups decreased with increasing heating temperatures. At temperatures >800 ^oC, almost all these bands disappeared, indicating that the functional groups of the carbon surface have been removed by the pyrolysis [39].

Petroleum pitch has been used as a low-cost raw material to produce carbon fibres [40]. A carbon fibres precursor made from petroleum pitch is first stabilized through a programmed thermal oxidation process and than carbonised at elevated temperature to form carbon fibres. Fundamental chemical changes

take place in the precursor carbon fibre during the stabilization and carbonisation process (Figure 29).

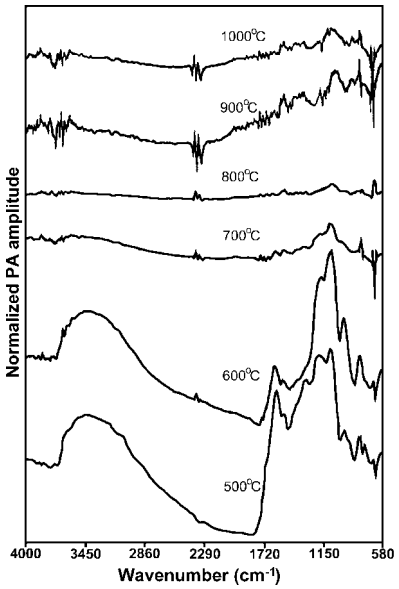

Fig. 28. FT-IR/Pas spectra of the adsorbent treated as a function of temperature range from 500 to 1000 ^{o}C [39]

The development of the hydroxyl bands (3450-3550 cm^{-1}) and the carbonyl band at 1697 cm^{-1} is observed during the first 40 min of the programmed stabilization process (Figure 29A a-c). This indicates that hydroxyl and carbonyls of ketone/aldehyde and carboxyl were the major oxidation products during this period of stabilization.

When the stabilization time was increased to 60 min, the intensities of the broad band around 3400 cm^{-1} due to hydrogen-bonded hydroxyl and the carbonyl band at 1697 cm^{-1} were significantly increased, whereas the intensities of the bands in the 3045-2864 cm^{-1} region due to the stretching of both saturated and unsaturated hydrocarbons, the bands in the 1444-1377 cm^{-1} region due to the bending of saturated aliphatic hydrocarbons, and the bands in the 870-750 cm^{-1} region due to the out-of plane bending of aromatic hydrocarbons were reduced (Figure 29A d). The 870 cm^{-1} band due to isolated aromatic C-H becomes weaker than the bands at 815 and 750 cm^{-1} in Figure 29A d. This reveals that the isolated hydrogens in the aromatic rings are easier to be oxidized than the other types of aromatic hydrogens in the carbon fibre. When the precursor carbon fibre was oxidized for 80 min, all those bands due to saturated hydrocarbons and aliphatic unsaturated hydrocarbons disappeared,

whereas the hydroxyl and carbonyl band intensities were further enhanced in the spectrum (Figure 29A f), indicating a complete oxidation of the precursor carbon fibre at the end of the stabilization process. The carbonyl band in Figure 29A f appears to be broad with its maximum at 1735 cm^{-1}, which is due to the stretching of ester carbonyl. The ester is probably the product of estrification between the hydroxyl and the carboxyl formed during the stabilization process.

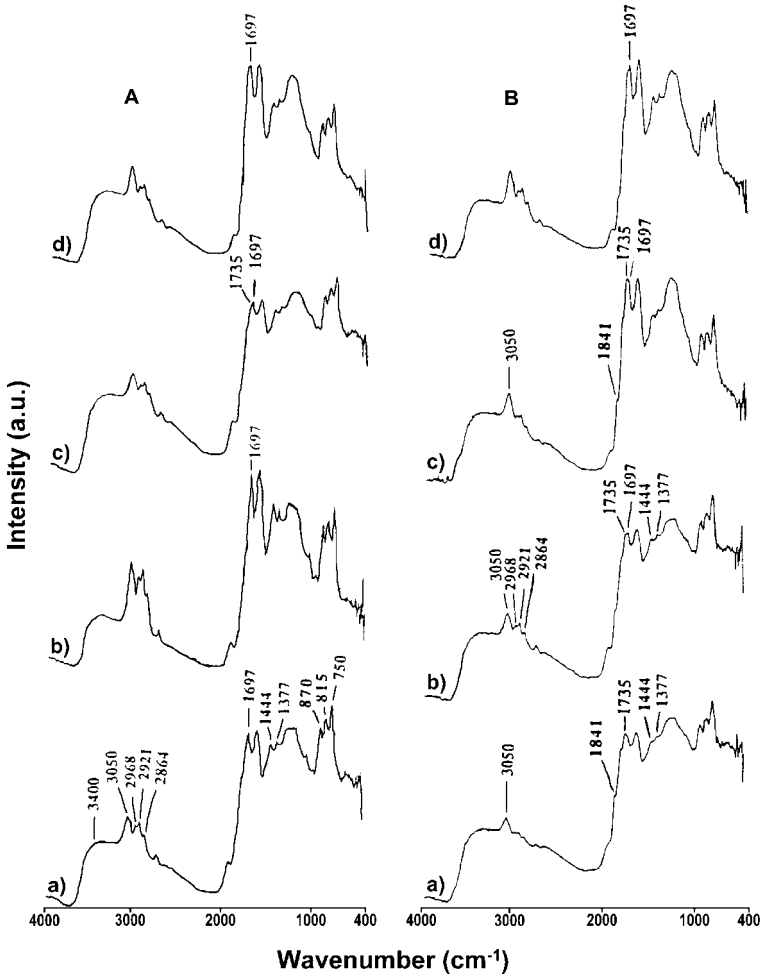

Fig. 29. FT-IR/PAS spectra of the precursor carbon fiber: A – stabilized, B – powder; stabilization time (min): a) 0, b) 20, c) 40, d) 60, e) 70, f) 80 [40]

The precursor carbon fibre at different stages of stabilization was ground into a powder. The FT-IR/PAS of the powder samples are shown in Figure 29B. It should be noticed, that FT-IR/PAS of the carbon fibre represents a few

micrometers' near surface of the fibre (Figure 29A). When the carbon fibre is ground into a powder, the surface and the bulk of the fibre is mixed (Figure 29B). As a result, a spectrum of the powder is mainly contributed by the bulk of the carbon fibre. The distribution of the oxidation products between the surface and the bulk of a carbon fibre can be determined by comparison of the spectrum of a fibre with that of a powder (Figs. 29A and B). Few differences are found between the spectra of carbon fibre stabilized for 0, 20, and 40 min (Figure 29A a-c) and the spectra of the corresponding powder samples (Figure 29B a-c), indicating a homogeneous distribution of the oxidation products between the surface and the bulk of the precursor carbon fibre in the first 40 min of stabilization. Differences start to appear in the spectrum of the fibre stabilized for 60 min (Figure 29A d) and the spectrum of the corresponding powder (Figure 29B d). The band at 870 cm^{-1} due to isolated aromatic C-H has lower intensity than the band at 815 cm^{-1} due to aromatic rings containing two adjacent hydrogens in the spectrum of the fibre (Figure 29A d), while the reverse is true in the spectrum of the corresponding powder (Figure 29B d). This is probably due to the fact that the isolated aromatic hydrogen has a higher degree of oxidation in the near surface of the fibre than in the bulk so that there is more reduction in the intensity of the 870 cm^{-1} band in Figure 29A d than in Figure 29B d.

Tab. 3. Functional groups and corresponding band frequencies in the investigated samples of carbon fibres [41].

Functional group	Band position (cm^{-1})
$-CH_3$ (mostly methyl substituents on aromatic rings)	2968, 2866,1444, 1377
$-CH_2$ (mostly methylene linkages linking aromatic rings)	2918, 2850*, 1478*
unsaturated aliphatic hydrocarbons	~3050*
aromatic rings	~3050, 1600
aromatic rings containing 4 adjacent hydrogens	750
aromatic rings containing 2 adjacent hydrogens	815
aromatic rings containing isolated hydrogens	870
C=O (aldehyde, ketone, carboxyl)	~1697
C=O (ester)	~1735*
C=O (anhydride)	~1841*
-OH (hydrogen bonded)	3450-3400
OH (free)	3550

*overlapped bands

Comparison of Figure 29A with Figure 29B reveals an inhomogeneous distribution of the oxidation products between the surface and the bulk in the fully stabilized precursor carbon fibre. At the end of the stabilization process, the near surface of the stabilized carbon fibre is completely oxidized, whereas the bulk of the fibre shows a lower degree of oxidation [40].

Three IR spectroscopic methods: FT-IR/PAS, DRIFTS, and TS, were evaluated for the qualitative analysis of carbon fibres [41]. The assignment of the bands in the IR spectra of the investigated carbon fibres is given in Table 3.

After the set of experiments, the band frequencies in the PAS, DRIFTS and TS spectra of the precursor carbon fibre stabilized for 20 min were summarized (Table 4).

Tab. 4. Band frequencies (cm^{-1}) in FT-IR/PAS, DRFTS and TS spectra of precursor carbon fiber stabilized for 20 min [41].

PAS*	DRFTS*	TS
3550	3545	-
3450	3446	-
3045	3047	3039
2968	2962	2957
2921	2918	2916
2864	2864	2856
1600	1604	1596
1444	1445	1438
1377	1377	1378
870	874	870
750	752	747

*determined on powdered fiber

The following conclusions were drawn:

- The TS method using a KBr pellet detects the bulk of a carbon fibre; in contrast, FT-IR/PAS and DRFTS methods differentiate the near-surface region of a carbon fibre from its bulk.
- The TS method suffers from interference by water in KBr pellets; extensive drying of a KBr pellet at elevated temperatures may cause chemical changes, so caution should be taken when collecting a transmission spectrum with a KBr pellet.
- FT-IR/PAS, DRFTS and TS spectra of carbon fibre have similar band frequencies; DRFTS and PAS techniques are reliable qualitative analysis techniques for carbon fibres.
- The PA method has a poor S/N (signal-to-noise) ratio, so requires a much longer data acquisition time than do the other two sampling methods.

4. CONCLUDING REMARKS

FT-IR/PAS is a complimentary technique to the other spectroscopic methods applied in surface science and catalytical investigations. It is applicable to nearly all samples encompassing a wide range of absorbance strengths and physical forms. This branch of spectroscopy is non-destructive, noncontact, applicable to macrosamples and microsamples, insensitive to surface morphology. PA is capable of measuring spectra of all types of solids without exposure to air or moisture. One of the advantages of this technique is relative low cost of the PA detector [9]. The disadvantage of the FT-IR/PAS is a limited possibility of *in situ* measurements [2,3], what is particularly of great importance in the catalytical investigations.

REFERENCES

[1] Boudart M., in *Handbook of heterogeneous catalysis*. Ed. G. Ertl, H. Knozinger, J. Weitkamp. Vol. 1, Wiley-VCH, Weinheim, Germany, 1997, pp 1-12.
[2] Ryczkowski J., *Catal. Today*, 68, 263 (2001) and references cited therein.
[3] Ryczkowski J., *Int. J. Vibr. Spec.*, [www.ijvs.com] 6, 2, 2 (2002).
[4] Weckhuysen B.M., *Chem. Commun.*, 97 (2002).
[5] http://www.harricksci.com/infoserver/Sampling%20Techniques/techniques.cfm
[6] Weaver M.J., *Topics Catal*., 8, 65 (1999).
[7] McClleland J.F., Bajic S.J., Jones R.W., and Seaverson L.M, in *Modern techniques in applied molecular spectroscopy*. Ed. F.M. Mirabella, John Wiley & Sons, Inc., Toronto, 1998, pp 221-265.
[8] McClleland J.F., Jones R.W., Luo S., and Seaverson L.M, in *Practical sampling techniques for infrared analysis*. Ed. P.B. Coleman, CRS Press, Boca Raton, 1993, pp 107-144.
[9] http://www.mtecpas.com
[10] McGovern S.J., Royce B.S.H., and Bezinger J.B., *Appl. Surf. Sci*., 18, 401 (1984).
[11] Eyring E.M., Riseman S.M., and Massoth F.E., in *Catalytic Materials: Relationship between structure and reactivity*, ACS Symp. Ser., Vol. 248, Washington, 1984, pp 399-410.
[12] Trajberg I., and Hansen T., *Spectrochim. Acta A*, 54, 1715 (1998).
[13] Noble D., Anal. Chem., 66, 757A (1994).
[14] Ryczkowski J., *Appl. Catal. A: General*, 110, N2 (1994).
[15] Ryczkowski J., *Appl. Catal. A: General*, 135, N2 (1996).
[16] Vidrine D.V., *Appl. Spectrosc*., 34, 314 (1980).
[17] Rockley M.G., *Appl. Spectrosc*., 34, 405 (1980).
[18] Ferraro J.R., in *Advances in materials characterization*. Ed. D.R. Rossington, R.A. Condrate and R.L. Snyder, Plenum Publishing, 1983, pp 171-198.
[19] Lai E.P.C, Chan B.L., and Hadjmohammadi M., *Appl. Spectrosc. Rev.*, 21, 179 (1985).
[20] Nyquist R.A., and Kagel R.O., *Handbook of infrared and Raman spectra of inorganic compounds and organic salts*, Vol. 4, Academic Press, Inc., 1997, pp 208-211.
[21] Benziger J.B., McGovern S.J., and Royce B.S.H., in *Catalyst Characterization Science*, ACS Symp. Ser. No. 288, Washington, 1985, pp 449-463.
[22] Poisson R., Brunelle J.-P., and Nortier P., in *Catalyst Supports and Supported Catalysts Theoretical and Applied Concepts*. Ed. A.B. Stiles, Butterworth, Boston, Mass., 1987, pp 11-55.

[23] Knözinger H., and Ratnasamy P., *Catal. Rev.-Sci. Eng*., 17, 31 (1978).
[24] Knözinger H., *Adv. Catal*., 25, 184 (1976).
[25] Carter J.L., Lucchesi P.J., Corneil P., Yates D.J.C., and Sinfelt J.H., *J. Phys. Chem*., 69, 3070 (1965).
[26] Peri J.B., *J. Phys. Chem*., 69, 220 (1965).
[27] Peri J.B., *J. Phys. Chem*., 69, 211 (1965).
[28] Dunken H., and Fink P., *Z. Chem*., 6, 194 (1966).
[29] Tsyganienko A.A., and Filimonov V.N., *J. Molec. Struct*., 19, 579 (1973).
[30] Skapin T., *J. Non-Cryst. Solids*, 285, 128 (2001).
[31] Nishikawa Y., Kimura K., Matsuda A., and Kenpo T., *Appl. Spectrosc*., 46, 1695 (1992).
[32] Ryczkowski J., Borowiecki T., and Nazimek D., *Adsorp. Sci. Technol*., 14, 113 (1996).
[33] Hess A., and Kemnitz E., *Appl. Catal. A: General*, 149, 373 (1997).
[34] Hess A., and Kemnitz E., *J. Catal*., 149, 449 (1994).
[35] Mohamed M.M., and Vansant E.F., *Colloids and Surfaces A: Physicochem. Engn. Aspects*, 96, 253 (1995).
[36] Mohamed M.M., *Spectrochim. Acta*, 51A, 1 (1995).
[37] El Shafei G.M.S., and Mokhtar M., *Colloids and Surfaces A: Physicochem. Engn. Aspects*, 94, 267 (1995).
[38] Pokrovskiy V.A., Leboda R., Turov V.V., Charmas B., and Ryczkowski J., *Carbon*, 37, 1039 (1999).
[39] Hu Z., and Vansant E.F., *Carbon*, 33, 1293 (1995).
[40] Simms J.R., and Yang C.Q., *Carbon*, 32, 621 (1994).
[41] Yang C.Q., and Simms J.R., *Fuel*, 74, 543 (1995).

CURRICULA VITAE

Dr Janusz Ryczkowski was born in Poland in 1959. Graduated from the Nicholas Copernicus University in Toruń (1983). Received his Ph.D. degree (1992) at the Maria Curie-Sklodowska University in Lublin. He is an official correspondent for Applied Catalysis News Brief (1994 -), member of Polish Chemical Society (1984 -), Polish Catalysis Club (1993 -). Besides, frequent short visits, he also made long-term stay to Central Research Institute of Chemistry of the Hungarian Academy of Sciences (Hungary) and Ecole National Superieure de Chimie de Lille (France). In the frame of Socrates Programme he has visited University of Limerick (Ireland) and University of Porto (Portugal) with a series of lectures. As for today he was a referee of the papers submitted to: Polish Journal of Chemistry, Journal Chemical Society of Pakistan, Pakistan Journal Society and Industrial Research, Vibrational Spectroscopy, Langmuir, and Applied Catalysis B: Environmental. On the request of the Authorities of Quaid-i-Azam University (Pakistan) since 1994 six times he was a referee of doctoral thesis. His main field of interest is preparation of mono- and bimetallic catalysts, catalyst's modification, their characterization, and application of infrared spectroscopy in catalytic research. He published over 65 papers. Recently, he published two reviews: in a special volume of Catalysis Today (2001), and in the Internet Journal of Vibrational Spectroscopy (2002).

Sylwia Pasieczna was born in Lublin, Poland in 1974. She studied chemistry at the Maria Curie-Skłodowska University, graduated in 1998. She is member of Polish Chemical Society (1998-) and Polish Catalysis Club (1998-). At present she is an assistant at the Department of Chemical Technology at M.C.S. University. Her main field of interest is application of infrared spectroscopy in catalytic and coal deposits research.